

## RESEARCH ARTICLE

# Particle-based simulation of bubbles in water–solid interaction

Xuqiang Shao\*, Zhong Zhou and Wei Wu

State Key Laboratory of Virtual Reality Technology and Systems, Beihang University No. 37, Xueyuan Road, Beijing 100191, China

## ABSTRACT

In this paper, a particle-based multiphase method for creating realistic animations of bubbles in water–solid interaction is presented. To generate bubbles from gas dissolved in the water on the fly, we propose an approximate model for the creation of bubbles, which takes into account the influence of gas concentration in the water, the solid material, and water–solid velocity difference. As the air particle on the bubble surface is treated as a *virtual nucleation site*, the bubble absorbs air from surrounding water and grows. The density and pressure forces of air bubbles are computed separately using smoothed particle hydrodynamics; then, the two-way coupling of bubbles with water and solid is solved by a new drag force, so the generated bubbles' flow on the surface of solid and the deformation in the rising process can be simulated. Additionally, touching bubbles merge together under the cohesion forces weighted by the smoothing kernel and velocity difference. The experimental results show that this method is capable of simulating bubbles in water–solid interaction under different physical conditions. Copyright © 2012 John Wiley & Sons, Ltd.

## KEYWORDS

bubbles; water–solid interaction; particle-based method; smoothed particle hydrodynamics

### \*Correspondence

Xuqiang Shao, State Key Laboratory of Virtual Reality Technology and Systems, Beihang University No. 37, Xueyuan Road, Beijing 100191, China.

E-mail: shaoxuqiang@gmail.com

## 1. INTRODUCTION

The interaction between water and solid is a natural phenomenon that occurs in everyday life; for example, a stone drops into the water. It can create complex and interesting motions that would be difficult to be animated convincingly by hand. Up to now, in computer graphics, many physically based methods have been proposed to simulate one-way or two-way fluid–solid interaction automatically. Apparently, the visual realism of water–solid interaction can be significantly enhanced by realistically simulating small-scale details such as droplets and bubbles. However, to our knowledge, it is still a challenge to model bubbles in water–solid interaction because bubbles should be coupled to the framework of fluid–solid interaction effectively.

There are mainly two approaches employed to model fluid–solid interaction, the coupled method and the unified particle-based method. In the coupled method, the variety of the simulated materials and effects are often constrained by the interfaces between the models, so bubbles are difficult to be coupled to this type of fluid–solid interaction framework. In contrast, the unified particle-based method simplifies the fluid–solid interaction in a unified way and is suitable for capturing small-scale effects such as droplets

and bubbles. Our method employs particle-based approach to simulate bubbles in fluid–solid interaction.

Although several methods [1–3] have been proposed to simulate bubbles in water–solid interaction, the generation and growth of bubbles are not well resolved. In this paper, we focus on the simulation of bubbles from the gas dissolved in the water. On the basis of the physics of dissolved gas diffusion and nucleation, our method generates bubbles as a cluster of smoothed particle hydrodynamics (SPH) particles surrounding the solid surface on the fly, and the influence of the gas concentration in the water, the solid material, and water–solid velocity difference on the generation of bubbles is taken into account. As the air particle on the bubble surface is treated as a *virtual nucleation site*, the bubble absorbs air from surrounding water and grows.

In the simulation of bubbles in water–solid interaction, air, water, and solid interact with each other in the two-way manner. In our method, because all three phases are simulated using SPH, the interaction seems to be calculated by the multiphase SPH method in [4]. Although the method in [4] can handle density ratios of up to 100, the very large density ratio of air to water ( $\approx 1000$ ) is problematic for multiphase SPH solvers. In contrast, we compute the density and pressure forces of air phase separately.

The two-way coupling of bubbles with water and solid is solved by a new drag force, so the generated bubbles' flow on the surface of solid and deformation in the rising process can be simulated. In addition, under the cohesion forces weighted by the smoothing kernel and velocity difference of air particles, bubbles touching with another merge together. Coupled with the volume-dependent buoyancy model in [5], our approach could simulate the complex bubble flow in water–solid interaction, for example, path instability, deformation and merging of bubbles, and foams.

The remainder of this paper is organized as follows. The next section reviews the related work in particle-based fluid–solid interaction and bubble simulation. Section 3 discusses our particle-based water–solid interaction framework. Sections 4 and 5 detail the proposed method for realistically simulating the bubbles from dissolved air in water–solid interaction. Section 6 gives the implementation flowchart and some animations created with the proposed method. Finally, this paper is concluded in the last section.

## 2. RELATED WORK

In this work, we focus on coupling air bubbles simulated by SPH to particle-based fluid–solid framework. In this section, we will review particle-based interaction and bubble simulation methods.

### 2.1. Particle-based Interaction Methods

Recently, several particle-based frameworks that unify simulation algorithms for fluid, solid, and interaction have been proposed. Müller *et al.* [6] proposed a fully particle-based technique to model elastic, plastic, and melting behavior of objects, where a moving least squares approach is used to calculate the elastic forces. Keiser *et al.* [7] enhanced the approach of Müller *et al.* [6]. In their approach, the Navier–Stokes equations are merged with the equations for deformable solids to handle the physical animation of solids, fluids, and phase transitions. Solenthaler *et al.* [8] used SPH to approximate the Jacobian of the deformation field, so coarsely sampled and coplanar particle configurations can be handled. The aforementioned researches mainly focus on the phase transition interaction. Iwasaki *et al.* [9] provided a particle-based method for the simulation of the melting and freezing of ice objects and the interactions between ice and water. In their work, to simulate the flow of meltwater on ice and the formation of water droplets, a simple interfacial tension is developed. Our previous work [10] presented a unified particle-based model to realistically simulate deformable solid–fluid interaction. In the method, the solid is treated as a special fluid constrained to solid motions, and deformable solid–fluid interaction could be computed directly by the multiphase SPH solver.

### 2.2. Bubble Simulation

Many methods have been proposed to simulate bubbles in the water. Because in Eulerian methods capturing the small-scale flow of bubbles requires very fine grid resolutions, pure grid-based methods such as the regional level set method [11,12] are only suited to handle relatively large bubbles in comparison to the fluid volume.

Bubbles are mainly simulated by a hybrid model in which air particles are coupled to the water solver. Kück *et al.* [13] simulated dynamic foams by simplifying bubbles into spherical particles, so they avoided the topology changing problem and focused on the interaction between bubbles and cluster behaviors. Hong and Kim [14] combined the volume-of-fluid and front-tracking methods to create particle bubbles emanating from entrapped air pockets, and handled the topological changes of bubble shape using surface tension. Greenwood and House [15] created bubbles by using level set marker particles and trapped air pockets but did not take into account the change of bubble shape. By coupling the bubble particles to a low-resolution grid, millions of air particles can be simulated efficiently in [16]. However, in these models, each bubble is treated as a sphere and the interaction of bubbles is often neglected. Therefore, the size and shape of air bubbles are not varying over time.

Because air bubble is a type of fluid, some hybrid solvers in which bubbles are simulated with Lagrangian particle method SPH have been proposed. In order to resolve sub-grid splashes, Foster *et al.* [17] used the SPH method to model escaped particles within the particle level set method [18]. Losasso *et al.* [19] improved this approach by coupling a model of dense water volume to diffuse sprays. In [20], bubbles are simulated with SPH and coupled to a grid-based fluid solver. The two phases are coupled via the velocity field. However, because of the insufficient resolution of the underlying grid, the path instability of air bubbles cannot be simulated. In [21], a particle-based bubble simulation is coupled to two-dimensional shallow water model. In order to capture three-dimensional effects, the shallow water model makes a number of simplifying assumptions. In particular, the fluid flow is only modeled around bubbles and only if bubbles are in the fluid. Although the model is very efficient to compute, some effects cannot be modeled, for example, inertia effects of the fluid.

Several unified particle-based methods have been presented to model air bubbles in water. In [22], the standard SPH model for single-phase fluid simulations [23] is extended to handle multiple fluids. This approach can handle density ratios of up to 10. In order to simulate air bubbles, an artificial buoyancy force is applied. However, this approach suffers from falsified density estimations at the interface, which induce wrong pressure values. Solenthaler *et al.* [4] overcame this problem by ignoring the mass in the computation of the particle density. Thereby, sharp density changes at the fluid interface can be reproduced. Although this method can handle density

ratios of up to 100, the flow of small, light volumes such as air bubbles cannot be realistically handled. In order to solve problems caused by large density ratios, Cleary *et al.* [24] proposed a method to simulate dynamic gas bubbles generated from gas dissolution, where each phase is computed separately. The bubbles modeled by discrete entities with fixed shape are coupled to the SPH liquid via a drag force, whereas the influence of the bubbles on the liquid is neglected. Markus *et al.* [5] ignored particle neighbors of other phases when computing the density. They treat each SPH-based phase separately, and the interaction of both phases is modeled via a drag force. Our method also computes SPH-based air bubbles separately, but we couple water, air bubbles, and solid in the two-way manner using a different formulation of the drag force, so the generated bubbles' flow on the surface of solid and deformation in the rising process can be simulated.

The aforementioned methods only couple air bubbles and water, and do not contain the solid phase. Mihalef *et al.* [2] proposed a new Eulerian method that couples gas and liquid with temperature-driven mass-transfer in boiling. They performed interactions of bubbles with static and heated solids. Bubbles are seeded at some randomly selected nucleation sites on the solid surface. Hong *et al.* [1] extended previous Eulerian grids fluid simulation techniques to incompressible viscous multiphase fluids, focusing on surface tension effects, viscosity changes at surfaces, and buoyancy. But in their method, they only simulated the interaction of formed bubbles with static solid sphere. Mihalef *et al.* [3] presented a new Eulerian–Lagrangian method for physics-based simulation of fluid flow, which includes automatic generation bubbles from trapped air in water–solid interaction. But their method does not take into account drag forces between bubbles. In this paper, we simulate bubbles from the gas dissolved in the water, mainly focusing on the generation of bubbles, the flow of bubbles on the solid surface, and bubble deformation and merging.

### 3. PARTICLE-BASED WATER–SOLID INTERACTION FRAMEWORK

The water–solid interaction is simulated based on our previous work [10]. In the method, by breaking down solids and fluids into particles with various properties, we use a unified particle-based model to simulate solids, fluids, and their interaction.

#### 3.1. SPH Method

In SPH, particles are used to interpolate a continuous function  $A(\mathbf{x})$  at a position  $\mathbf{x}$ . The contributing particles, relevant for a position, are determined by a kernel function  $W$  of finite support radius  $h$  associated with each particle. The

interpolation is given as

$$A(\mathbf{x}_i) = \sum_j m_j \frac{A_j}{\rho_j} W(\mathbf{x}_{ij}, h) \quad (1)$$

where  $m_j$  is the mass of neighboring particle  $j$ ,  $A_j$  the function value at the position  $\mathbf{x}_j$ ,  $\rho_j$  its density, and  $\mathbf{x}_{ij} = \mathbf{x}_i - \mathbf{x}_j$  the position vector from particle  $i$  to particle  $j$ .  $W(\mathbf{r}, h)$  is a smoothing kernel, which is typically a smooth, radially symmetric, normalized function with finite support radius  $h$ , that is,  $\int W(\mathbf{r}, h) d\mathbf{r} = 1$  and  $W(\mathbf{r}, h) = 0$  for  $|\mathbf{r}| > h$ .

In fluid and solid equations, derivatives of field quantities appear and need to be evaluated. With the SPH approach, the derivatives only affect the smoothing kernel. The gradient and Laplacian of the smooth attribute function  $A(\mathbf{x})$  are

$$\nabla A(\mathbf{x}_i) = \sum_j m_j \frac{A_j}{\rho_j} \nabla W(\mathbf{x}_{ij}, h) \quad (2)$$

$$\nabla^2 A(\mathbf{x}_i) = \sum_j m_j \frac{A_j}{\rho_j} \nabla^2 W(\mathbf{x}_{ij}, h) \quad (3)$$

#### 3.2. Fluid and Solid Simulation

Our SPH fluid framework is based on the work of [22,23,25]. Fluid behavior is modeled by the Navier–Stokes equation

$$\frac{d\rho}{dt} = -\rho \nabla \cdot \mathbf{v} \quad (4)$$

$$\rho \frac{D\mathbf{v}}{Dt} = -\nabla P + \mu \nabla^2 \mathbf{v} + \mathbf{f} \quad (5)$$

where  $\mathbf{v}$  is velocity,  $P$  pressure,  $\mu$  viscosity coefficient, and  $\mathbf{f}$  represents the external force. Equation (4) is momentum equation and Equation (5) mass equation.

Applying Equation (1) to the density of a particle  $p_i$  at location  $\mathbf{x}_i$  yields the so-called summation density

$$\rho_i = \rho(\mathbf{x}_i) = \sum_j m_j W(\mathbf{x}_{ij}, h) \quad (6)$$

Substituting Equations (2) and (3) into the Navier–Stokes momentum equation and symmetrization yield the following pressure and viscosity forces acting on a particle  $p_i$

$$\mathbf{F}_i^{\text{pressure}} = - \sum_j m_j \frac{P_i + P_j}{2\rho_j} \nabla W(\mathbf{x}_{ij}, h) \quad (7)$$

$$\mathbf{F}_i^{\text{viscosity}} = \mu \sum_j m_j \frac{\mathbf{v}_j - \mathbf{v}_i}{\rho_j} \nabla^2 W(\mathbf{x}_{ij}, h) \quad (8)$$

We use the kernels  $W(\mathbf{r}, h)$  described in [23]. The pressure  $P_i$  is computed via the Tait’s equation in [25]

$$P_i = \frac{K\rho_0}{\gamma} \left( \left( \frac{\rho_i}{\rho_0} \right)^\gamma - 1 \right) \quad (9)$$

where  $K$  is the stiffness of the fluid,  $\rho_0$  the rest density, and  $\gamma$  is set to 7 to enforce low-density variations.

Rigid solid objects are simulated as described in [8]. The rigid body is sampled with particles, and forces acting on these particles are accumulated to a total force and torque on the body to enforce rigid body motion.

In order to constrain the motion of an object to rigid body motion, we have to handle rotation explicitly. To do so, we compute a torque vector  $\tau$  as

$$\tau_i = (\mathbf{r}_i - \mathbf{r}^{\text{cm}}) \times \mathbf{F}_i \quad (10)$$

where  $\mathbf{r}^{\text{cm}}$  is the center of mass of a body and  $\mathbf{F}_i$  denotes the total force exerted on the  $i$ th particle.

The total force acting on a rigid body is given by  $\mathbf{F}_{\text{total}} = \sum_i \mathbf{F}_i$  and the total torque is defined by  $\tau_{\text{total}} = \sum_i \tau_i$ . Then, time integration is performed by iterating over a rigid object to calculate the effect of the force and torque, that is, the effect on the position and the linear and angular velocity of the object.

### 3.3. Water–Solid Interaction

As shown in Figure 1, in the fluid–solid interaction simulation, there are three types of forces between particles to be calculated: the force between fluid particles  $\mathbf{F}^{\text{fluid–fluid}}$ , force between solid particles  $\mathbf{F}^{\text{solid–solid}}$ , and interaction force between solid and fluid particles  $\mathbf{F}^{\text{solid–fluid}}$ . In our particle-based model, based on the work of [26], we treat each solid object as a special fluid constrained to solid’s motions; thus, the two-way interaction can be achieved directly by solving the governing equations of fluid using multiphase SPH method.  $\mathbf{F}^{\text{fluid–solid}}$  is solved in the same way as  $\mathbf{F}^{\text{fluid–fluid}}$ , which is the summation of  $\mathbf{F}^{\text{pressure}}$  and  $\mathbf{F}^{\text{viscosity}}$  calculated by Equations (7) and (8).  $\mathbf{F}^{\text{solid–solid}}$  is the force between neighbor particles from different solid objects. Still solved in the same way as  $\mathbf{F}^{\text{fluid–fluid}}$ ,  $\mathbf{F}^{\text{solid–solid}}$  is responsible for interactions between solid objects.

The solid described in this paper is impermeable, and only relying on the aforementioned interaction, forces between particles cannot overcome leaks. In order to prevent the fluid penetrating into solid, a straightforward detection and velocity correction method presented in [27] is employed. Through modifying the velocity of fluid particles adjacent to the solid to the velocity of solid particle, the coming penetration can be avoided simply.

However, the density summation Equation (6) for fluid–solid interaction based on multiphase SPH will become problematic when a particle has neighbor particles with

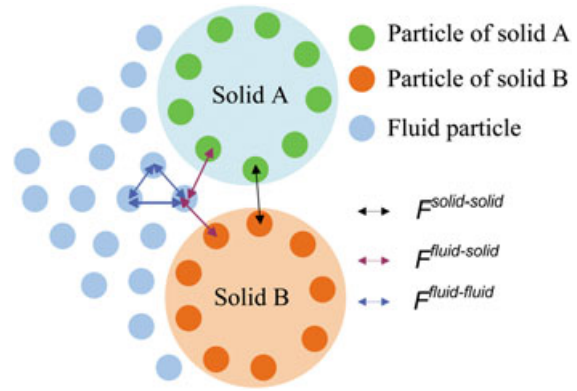


Figure 1. Forces between solid and fluid particles.

different rest densities. Either overestimating or underestimating the density will lead to erroneous pressure values, which might result in unnatural acceleration caused by erroneously introduced pressure ratios. To handle density discontinuities at interfaces between fluid and solid correctly, we replace the density summation formulated as Equation (6) by a different density model used in [4]. The idea is to make each particle treat its neighbors as if they would have the same rest density and mass as itself. The density model is defined as

$$\tilde{\rho}_i = m_i \delta_i = m_i \sum_j W(\mathbf{x}_{ij}, h) \quad (11)$$

Substituting the new density  $\tilde{\rho}$  into Equations (7), (8), and (9), we get the new formulation of pressure, pressure forces, and viscous forces. With the modified density, pressure, and force equations, we are able to eliminate all spurious and unnatural interface tension effects and simulate fluid–solid interaction with large density ratios of up to 100.

### 4. BUBBLE GENERATION

During fluid–solid interaction such as a ball dropping into water, a bubble is formed at a nucleation site on the solid surface when enough gas has been transported by water to the site to form a bubble of the minimum critical size. The main source of bubbles is the gas dissolved in water, so the number of bubbles generated is influenced by the gas concentration  $C$  in water. For example, carbonated drinks such as Sprite generate more bubbles than mineral water. The generation of bubbles also depends on the solid surface conditions like roughness and adsorbability. Moreover, the velocity difference between water and solid also influences the generation of bubbles. In our simulations, all of the aforementioned factors influencing the formation of bubbles are taken into account to generate air particles only where needed on the fly.

For bubble generation, the air particles are seeded on some selected nucleation sites on the solid surface. In the

preprocessing stage, we select the surface particle whose curvature radius is greater than a threshold value as a nucleation site. According to bubble nucleation theory, the threshold value is 0.2 μm. The curvature radius is the reciprocal of the interfacial curvature, which can be accurately calculated by the stable and accurate curvature method proposed in our previous work [10].

In our particle-based water–solid interaction, each water particle represents a volume of water, and carries its dissolved gas with it wherever it goes. The selected nucleation sites on the solid surface will gather air diffused from neighbor water particles to form bubbles. For a nucleation site surrounded by water particles, the rate change of gas concentration is

$$\frac{\partial C_i}{\partial t} = H_s \sum_j C_j \frac{\|v_j - v_i\|}{\|x_{ij}\|^2 + \epsilon^2} \nabla^2 W(x_{ij}, h) \quad (12)$$

where  $C_j$  is the gas concentration of the  $j$ th neighbor water particle,  $H_s$  is a solid material property parameter,  $\epsilon$  is a small parameter used to smooth out the singularity at  $\|x_{ij}\| = 0$ , and  $W$  is a smoothing kernel function, which is the same as that used for computing viscosity, as proposed in [23].

The number of generated air particles for a nucleation site is the ratio between the gas concentration and air particle mass. The position and velocity of the generated air particle are chosen to be the same as the values of the nucleation site on the solid surface.

When bubbles move, they grow by collecting more gas from the nearby water. The rate of bubble growth is controlled by the amount of gas that is diffused from neighboring water particles. In our method, we treat the air particle on the surface of bubble as a virtual nucleation site, the rate change of gas concentration is also calculated by Equation (12). But the position of generated air particle, as illustrated by Figure 2, is set to the coordinate of the point whose distance to virtual nucleation site along the surface normal is the rest spacing  $d$  between air particles.

The gas dissolved in water will diffuse. In our method, according to a conventional diffusion equation solved on the SPH particles, the rate of change of gas concentration

for a water particle  $i$  is

$$\frac{\partial C_i}{\partial t} = \sum_{j \in N_i} \kappa m_j \frac{(C_j - C_i)}{\rho_j} \nabla^2 W(x_{ij}, h) \quad (13)$$

where  $\kappa$  is the diffusivity of the gas in the water.

## 5. BUBBLE PHYSICS

In order to simulate realistic bubbles in water–solid interaction, we have to capture the prominent effects of their complex behaviors. When bubbles are formed at the nucleation site on the solid surface, they will move along the solid surface under the influence of solid and water before detaching from the solid surface. Bubbles deform in the rising process and have unstable path. In general, bubbles whose shapes are like spheres will merge together according to cohesion forces (surface tension). Furthermore, bubbles are different in size, where larger bubbles rise faster and attract smaller bubbles. For modeling these effects, the coupling of the three phases is realized by the drag force  $F^{drag}$ . We employ two forces that are computed for the air phases only, namely the buoyancy force  $F^{buoyancy}$  and the cohesion force  $F^{cohesion}$ .

### 5.1. Interaction

In our method, air bubbles simulated with SPH are coupled to particle-based water–solid interaction framework where the solid object is treated as a special fluid constrained to solid’s motions. It seems that the interaction of bubbles with water and solid can be solved by multi-phase SPH method. For SPH-based multiple fluids with large density ratios, the density model proposed in [4] overcomes falsified density estimations at the interface by ignoring the mass in the computation of the particle density. Thereby, sharp density changes at the interface can be reproduced. This method can handle density ratios of up to 100, which is enough for the density ratio of water to solid. But because of the very large density ratio of water to air ( $\approx 1000$ ), the flow of small, light volumes such as air bubbles cannot be realistically handled. The buoyant volumes cannot break up the crystallized particle configuration formed by the pressure forces.

In order to circumvent these problems, similar to [5], we propose to simulate the air phase separately using SPH; that is, only particle neighbors of the same phase contribute to the density of air particle. The generated bubbles often move along the solid surface before detaching from it and deform in the rising process. To simulate this behavior, as shown in Figure 3, the interaction of bubbles with water and solid is modeled via a new drag force that is related to velocity difference, the distance between particles, and the material coefficient of water and solid. The drag force is

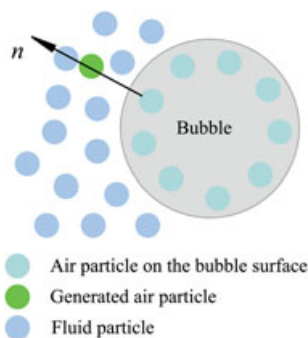


Figure 2. The growth of bubbles.

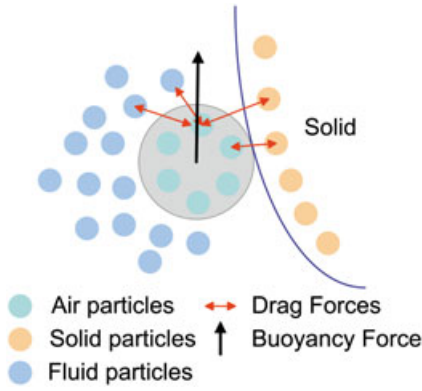


Figure 3. The proposed drag forces.

defined as

$$\mathbf{F}_i^{\text{drag}} = \sum_{j \in N_i^w} K_w m_j \frac{\mathbf{v}_{ij} \cdot \mathbf{x}_{ij}}{\|\mathbf{x}_{ij}\|^2 + \varepsilon^2} \nabla W(\mathbf{x}_{ij}, h) + \sum_{k \in N_i^s} K_s m_k \frac{\mathbf{v}_{ik} \cdot \mathbf{x}_{ik}}{\|\mathbf{x}_{ik}\|^2 + \varepsilon^2} \nabla W(\mathbf{x}_{ik}, h) \quad (14)$$

where  $j$  is the index of neighbor water particle,  $k$  is the index of neighbor solid particle,  $\mathbf{v}_{ij}$  and  $\mathbf{v}_{ik}$  are velocity differences between neighboring particles,  $W$  is the interpolation kernel,  $\varepsilon$  is a small parameter used to smooth out the singularity at  $\|\mathbf{x}_{ij}\| = 0$ ,  $K_w$  is the coefficient of water, and  $K_s$  is the coefficient of solid surface material.

The drag force is incorporated into the external force  $\mathbf{f}$  in motion equation formulated as Equation (4). In [20,24], the air bubbles are also coupled to the liquid phase via an empirical drag force, but the effect of bubbles on the liquid phase is neglected. Compared with the method in [5], the drag force that we used is related to the material coefficient of water and solid, which is suitable for simulating bubbles in water–solid interaction under different physical conditions.

### 5.2. Cohesion Forces

Unlike large-scale phenomena, small details such as bubbles are dominated by surface tension. The coalescence of air bubbles is an important effect. As shown in Figure 4, air bubbles are attracted by surrounding bubbles and merge together because of surface tension forces. Inspired by a microscopic view that, on a molecular level, surface tension arises as a result of attractive forces between molecules, we propose a new surface tension model that relies on cohesion forces. The approach is closely related to the cohesion forces for bubbles proposed in [5]. In contrast to their method, we not only scale the attractive forces using the smoothing kernel  $W$  as a weighting function, but also consider the influence of velocity difference between

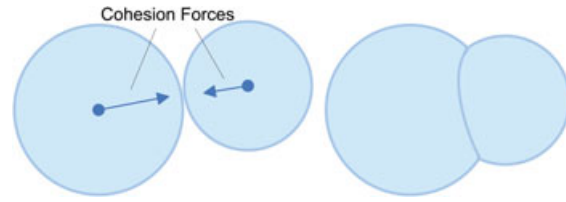


Figure 4. Cohesion forces acting on touching bubbles.

air particles. The new cohesion force is given as

$$\mathbf{F}_i^{\text{cohesion}} = -K_c m_i \sum_j m_j (\mathbf{v}_{ij} \cdot \mathbf{x}_{ij}) W(\mathbf{x}_{ij}, h) \quad (15)$$

where  $K_c$  is a user-defined coefficient controlling the strength of the cohesion forces.

The attractive forces between bubbles can be computed efficiently by using Equation (15). Air particles are attracted by neighboring particles of the same phase; thus, spatially close air bubbles merge together. When the density  $\rho_i$  of air particle becomes too high, the pressure force formulated as Equation (7) will counteract the attraction. As a result, the surface of the bubble is minimized while the forces converge to an equilibrium.

### 5.3. Buoyancy and Foam

The buoyancy force accelerates the air bubble in direction of the water surface. When air bubbles reach the water surface, they do not rise anymore, but float on the water surface and create foam structures before they burst. In our work, the calculation of buoyancy and foam is based on the methods proposed by Markus *et al.* [5].

In order to make larger bubbles rise faster than smaller ones, Markus *et al.* [5] related the magnitude of the buoyancy force to the number of particle neighbors  $n$ . In addition, we take into account the effect of water–gas density difference on the buoyancy force. The new calculation formula of buoyancy force is

$$\mathbf{F}_i^{\text{buoyancy}} = -m_i k_b (k_{\text{max}} - (k_{\text{max}} - 1) \cdot e^{-0.1n_i}) \times (\rho_0^{\text{water}} - \rho_0^{\text{air}}) \mathbf{g} \quad (16)$$

where  $k_b$  controls the minimum buoyancy,  $k_{\text{max}}$  controls the maximum buoyancy, and  $\mathbf{g}$  is the gravity acceleration. The mass is added to the force formulation, in order to make the resulting acceleration independent of the simulation resolution. Thus, the resulting acceleration caused by the buoyancy force can be perfectly controlled because  $\|k_b \mathbf{g}\| \leq \|\mathbf{a}_i^{\text{buoyancy}}\| \leq \|k_{\text{max}} k_b \mathbf{g}\|$ .

A simplified foam model in [5] is used to simulate the floating and bursting of foam bubbles. The model firstly differentiates between the rising bubble particles and the

foam particles that are on the water surface. We can determine the water surface by comparing the number of particle neighbors with a given threshold. An air particle  $i$  is regarded to be on the water surface if there is no water neighbor  $j$  with  $\mathbf{x}_{ji} \cdot \mathbf{g} > 0$ . The buoyancy force of foam particles is computed as

$$\mathbf{F}_i^{\text{buoyancy}} = -m_i \mathbf{g} \quad (17)$$

The acceleration of foam particles due to gravity is canceled out by this buoyancy force. The foam particles are coupled to the water by the drag force formulated as Equation (14). But different with rising bubble particles, they do not suffer from the drag forces exerted by solid objects. Thereby, the resulting velocity of foam particles is governed by the surrounding water. Thus, the foam floats on the water surface. Because of the cohesion force, foam particles also cluster on the surface, trying to minimize the surface. Consequently, foam bubbles are different in size and shape.

When the rising bubble particle reaches the surface and changes to a foam particle, it is given a floating time  $t_f$ , that is, time until the particle is deleted. In order to improve the realism, we vary  $t_f$  for each particle randomly using a uniform distribution. However, if two foam particles merge, the minimum of their floating time is assigned to both particles. Thereby, foam bubbles consisting of more than one particle disperse at once.

## 6. IMPLEMENTATION AND RESULTS

To simulate bubbles in water–solid interaction, firstly, the rigid, water, and air particles configuration is initialized. For each particle, we do neighborhood search accelerated by uniform spatial hashing algorithm. Then, the governing equations of solid and fluid, and water–solid interaction are solved as described in Section 3. The air bubbles are coupled to water and solid by the proposed drag forces formulated as Equation (14). Then, the cohesion force is calculated by Equation (15). Buoyancy and the foam model for air bubbles are computed according to Equations (16) and (17). After the total force exerting on each particle is calculated, all particles are integrated to the next time step by using the leap-frog integration scheme. Finally, according to the updated positions and velocities of particles, the gas transfer amount is computed by Equations (12) and (14), and the air particles are generated. The flowchart of our system is described in Figure 5.

We have implemented our new method for the simulation of bubbles in water–solid interaction and used it to produce some example animations to demonstrate various bubble effects. The simulation and rendering parts of our system are implemented on a Microsoft Windows XP PC with dual Intel Core 2.8 GHz CPUs, 2.0 GB RAM, and NVIDIA GeForce GTX 480 GPU. For rendering, we use POV-Ray 3.6 to render triangle meshes extracted from a scalar field by the Marching Cube method [23]. The cell

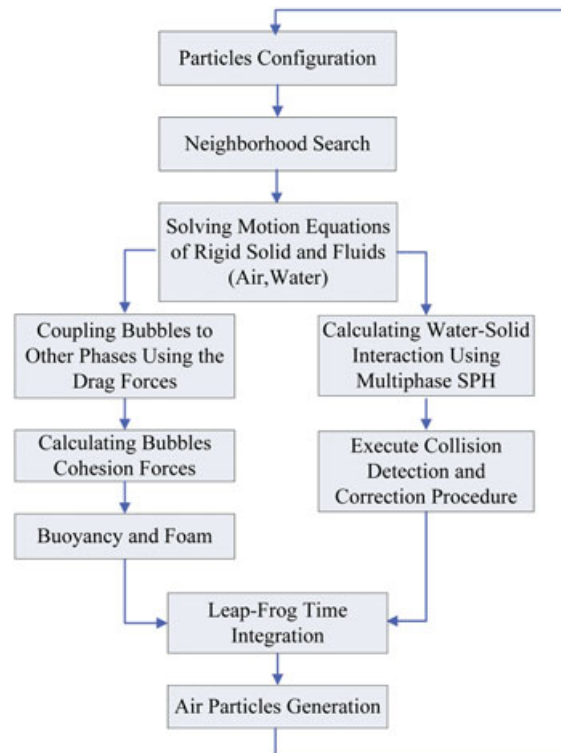


**Figure 5.** Flowchart of the simulation of bubbles in water–solid interaction. SPH, smoothed particle hydrodynamics.

size for the Marching Cube method is set to  $0.7d$ , and  $d$  is the rest particle spacing.

In all our example animations, we set the reference density of water to  $1000 \text{ kg/m}^3$ , and for air particles, we set it to  $1.25 \text{ kg/m}^3$ . The gravity is set to  $(0, -9.8, 0)^T$ . Velocities and accelerations are given in  $\text{m/s}$  and  $\text{m/s}^2$ , respectively. The gas concentration in water is given in  $\text{kg/m}^3$ . For example, the gas concentration of Sprite is  $6.03 \text{ kg/m}^3$ , beer  $3.96 \text{ kg/m}^3$ , and mineral water  $1.25 \text{ kg/m}^3$ . The hydrophilicity of solid material is measured by the contact angle made by a drop of water with a solid at the point of intersection. In our method, the size of the contact angle is used as the value of  $H_s$  in Equation (12). We use three different material solids: steel  $H_s = 75$ ,  $\rho = 7.9 \times 10^3 \text{ kg/m}^3$ ; aluminum  $H_s = 90$ ,  $\rho = 2.7 \times 10^3 \text{ kg/m}^3$ ; nylon  $H_s = 120$ ,  $\rho = 1.15 \times 10^3 \text{ kg/m}^3$ . For the example scenes,  $40k$  water particles and  $5k$  solid particles are used, and the maximum number of air particles is up to  $10k$ . The time step is set to  $0.003s$ , and the average CPU time per frame is  $7.6s$ .

In multiphase SPH, the fluid flow is mainly governed by the density computation. If the density ratio exceeds 10, the standard density summation Equation (6) will lead to erroneous pressure ratios that might result in unnatural acceleration. The density summation Equation (11) can handle density ratios of up to 100, which is suitable for water–solid interaction. However, the buoyancy of small,

light bubbles is significantly damped because of the pressure force, which compels the particles to arrange in a stable lattice structure. In contrast, our method simulates the air phase separately using SPH; that is, only particle neighbors of the same phase contribute to the air particle density. We couple bubbles with water and solid via a new drag force formulated as Equation (14), which does not take into account the density ratio and directly calculates the interaction forces on particle level. So, the problems induced by

large density ratio can be avoided. Figure 6 shows that the aluminum apple at a velocity of 10 m/s drops into water of gas concentration  $6.03 \text{ kg/m}^3$ . The air bubbles generated at the nuclear sites flow on the surface of steel apple, under the proposed drag forces, and grow because of the air absorbed from surrounding water. Moreover, the bubbles deform in the rising process, under the action of drag forces, and merge together because of the cohesion forces. When reaching the water surface, the bubbles float on the

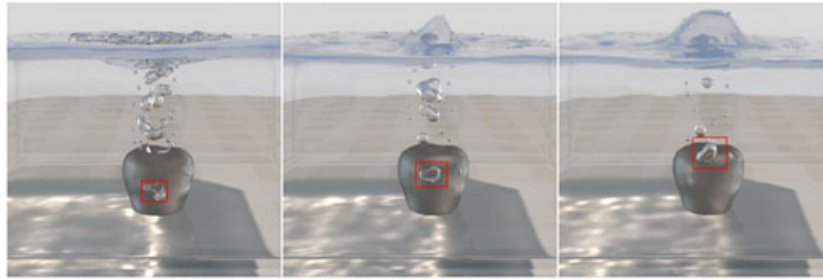


**Figure 6.** The generated bubbles' flow on the solid surface and grow.

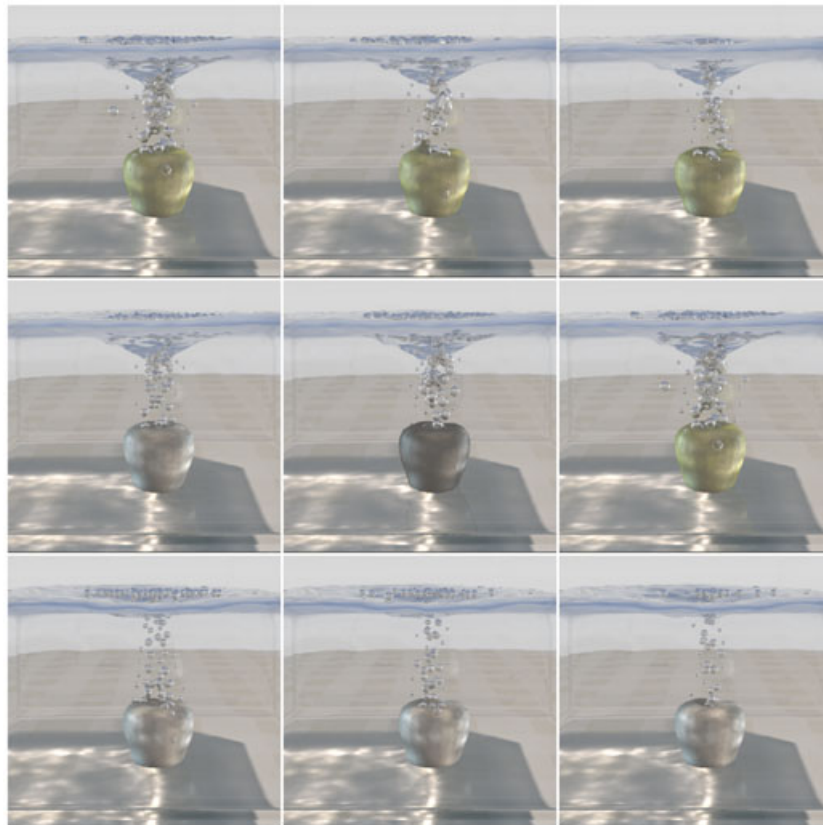


**Figure 7.** Top: the nylon solid apple at a velocity of 5 m/s drops into water of different gas concentrations,  $6.03 \text{ kg/m}^3$  (left),  $3.96 \text{ kg/m}^3$  (middle), and  $1.25 \text{ kg/m}^3$  (right). Middle: three different material solid apples at the same velocity 5 m/s drop into water of gas concentration  $6.03 \text{ kg/m}^3$ , steel (left), aluminum (middle), and nylon (right). Bottom: the steel solid apple drops into water of gas concentration  $6.03 \text{ kg/m}^3$  at different velocities, 10 m/s (left), 5 m/s (middle), and 3 m/s (right).

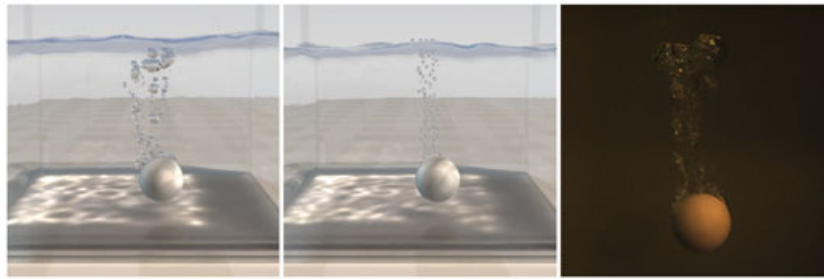


**Figure 8.** Comparison of bubble generation. Our method (left), Mihalef's method (middle), and the real phenomenon (right).

water surface in different sizes and shapes, according to the buoyancy, cohesion, and drag force.

Figure 7 shows the simulation of bubbles in water–solid interaction under different physical conditions such as gas concentration in the water, the solid material and water–solid velocity difference. The first row of Figure 7 shows the nylon solid apple drops into water of different gas concentrations:  $6.03 \text{ kg/m}^3$  (left),  $3.96 \text{ kg/m}^3$  (middle), and  $1.25 \text{ kg/m}^3$  (right). The velocity of solid apple dropping into water is 5 m/s. The second row shows different material solid apples at the same velocity 5 m/s drop into the water of the same gas concentration  $6.03 \text{ kg/m}^3$ : steel (left), aluminum (middle), and nylon (right). In the bottom row of Figure 7, the steel solid apple drops into water of the same gas concentration  $1.25 \text{ kg/m}^3$  at different velocities: 10 m/s (left), 5 m/s (middle), 3 m/s (right).

Figure 8 shows the generated bubbles of our method, Mihalef's method [3] and the real phenomenon. Compared with the most relevant Mihalef's method, our bubble model can simulate the growth of bubbles. In our method, because the two-way coupling of bubbles with water and solid is solved by a new drag force, the generated bubbles' flow on the surface of solid and deformation in the rising process can also be simulated. From the results, our method seems to be more approximating the real phenomenon.

Although our method can simulate physically plausible bubbles in water–solid interaction, it still has several limitations. First of all, based on the physics of dissolved gas diffusion and nucleation, we only focus on creating bubbles from the gas dissolved in the water on the fly. In fact, the trapped air is also the source of bubbles in water–solid interaction. However, this problem can be solved by combining our method with the bubble model proposed in [5]. Secondly, our method does not handle the vorticity of air particles. To simulate the motion of bubbles in more detail, we can incorporate the modification of SPH vorticity confinement method in [20] into our framework.

## 7. CONCLUSION

In this paper, for realistically simulating small-scale details in water–solid interaction, we have systematically developed a particle-based method capable of creating animations of bubbles from the gas dissolved in the water on the

fly. An approximate model, which considers the influence of gas concentration in the water, the solid material, and water–solid velocity difference on bubbles generation, has been put forward to create bubbles. As the air particle on the bubble surface is treated as a virtual nucleation site, the bubble collects air from surrounding water and grows. The two-way coupling of bubbles with water and solid is calculated by a new drag force, so the generated bubbles' flow on the surface of solid and deform in the rising process. The experimental results demonstrate that our method for bubble simulation can enhance the overall realism of water–solid interaction. The proposed method includes a significant amount of real physics, which enables users to create bubbles in water–solid interaction under different physical conditions without having to specify large numbers of artificial controls. Moreover, the bubble model can be implemented easily and integrated with existing particle-based water–solid framework.

Some immediate future works to further extend our method are as follows. First, to make the result more approximating the real phenomenon, we will try to take into account more factors affecting the bubble generation such as trapped air. Second, the particle-based method can be implemented with techniques on general-purpose computation on graphics processing units to increase the performance.

## ACKNOWLEDGEMENTS

This work is supported by the National 973 Program of China (grant no. 2009CB320805), the Natural Science Foundation of China (grant no. 61073070), the National 863 Program of China (grant no. 2012AA011803), and Fundamental Research Funds for the Central Universities of China.

## REFERENCES

- Hong JM, Kim CH. Discontinuous fluids. *ACM Transactions on Graphics (Proceedings of the 2005 ACM SIGGRAPH)* 2005; **24**: 915–920.
- Mihalef V, Unlusu B, Metaxas D, Sussman M, Hussaini MY. Physics-based boiling simulation. In *Proceedings of the 2006 Eurographics/ ACM*

- SIGGRAPH Symposium on Computer Animation*, Vienna, Austria, 2006.
3. Mihalef V, Metaxas D, Sussman M. Simulation of two-phase flow with sub-scale droplet and bubble effects. In *Proceedings of the 2009 Eurographics*, Munich, Germany, 2009; 28.
  4. Solenthaler B, Pajarola R. Density contrast SPH interfaces. In *Proceedings of the 2008 Eurographics/ACM SIGGRAPH Symposium on Computer Animation*, Dublin, Ireland, 2008; 211–218.
  5. Ihmsen M, Bader J, Akinci G, Teschner M. Animation of air bubbles with SPH. In *Proceedings of the 2011 International Conference on Computer Graphics Theory and Applications*, Vilamoura, Algarve, Portugal, 2011.
  6. Müller M, Keiser R, Nealen A, Pauly M, Gross M, Alexa M. Point based animation of elastic, plastic and melting objects. *Proceedings of the 2004 Eurographics/ACM SIGGRAPH Symposium on Computer Animation*, Grenoble, France, 2004; **14**: 141–151.
  7. Keiser R, Adams B, Gasser D, Bazzi P, Gross M. A unified lagrangian approach to solid–fluid animation. *Proceedings of the 2005 Symposium on Point-Based Graphics*, Stony Brook, NY, USA, 2005; **31**: 125–131.
  8. Solenthaler B, Schlaflfi J, Pajarola R. A unified particle model for fluid–solid interactions. *Computer Animation and Virtual Worlds* 2007; **18**(1): 69–82.
  9. Iwasaki K, Uchida H, Dobashi Y, Nishita T. Fast particle-based visual simulation of ice melting. *Computer Graphics Forum (Proceedings of the 2010 Pacific Graphics)* 2010; **29**: 2215–2223.
  10. Shao XQ, Zhou Z, Wu W. Unified particle-based simulation of deformable solid–fluid interaction. In *Proceedings of the 2011 Computer Graphics International*, Ottawa, Ontario, Canada, 2011.
  11. Zheng W, Yong JH, Paul JC. Simulation of bubbles. *Proceedings of the 2006 ACM SIGGRAPH/Eurographics Symposium on Computer Animation*, Vienna, Austria, 2006; **9**: 325–333.
  12. Song O, Shin H, Ko HS. Stable but non-dissipative water. *ACM Transactions on Graphics* 2005; **24**: 81–97.
  13. Kuck H, Vogelgsang C, Greiner G. Simulation and rendering of liquid foams. In *Proceedings of the 2002 Graphics Interface*, Calgary, Alberta, 2002; 81–88.
  14. Hong JM, Kim CH. Animation of bubbles in liquid. *Computer Graphics Forum* 2003; **22**: 253–262.
  15. Greenwood ST, House DH. Better with bubbles: enhancing the visual realism of simulated fluid. In *Proceedings of the 2004 ACM SIGGRAPH/Eurographics Symposium on Computer Animation*, Grenoble, France, 2004; 287–296.
  16. Kim D, Song OY, Ko HS. A practical simulation of dispersed bubble flow. In *Proceedings of the 2010 ACM SIGGRAPH*, Los Angeles, California, USA, 2010; 701–705.
  17. Foster N, Fedkiw R. Practical animation of liquids. In *Proceedings of the 2001 ACM SIGGRAPH*, Los Angeles, California, USA, 2001; 23–30.
  18. Enright D, Fedkiw R, Ferziger J, Mitchell I. A hybrid particle level set method for improved interface capturing. *Journal of Computational Physics* 2002; **183**(1): 83–116.
  19. Losasso F, Talton J, Kwatra N, Fedkiw R. Two-way coupled SPH and particle level set fluid simulation. *Journal of IEEE Transaction on Visualization and Graphics* 2008; **14**(4): 797–804.
  20. Hong JM, Lee HY, Yoon JC, Kim CH. Bubbles alive. In *Proceedings of the 2008 ACM SIGGRAPH*, Los Angeles, California, USA, 2008; 1–4.
  21. Thurey N, Sadlo F, Schirm S, Muller F, Gross M. Real-time simulations of bubbles and foam within a shallow water framework. In *Proceedings of the 2007 ACM SIGGRAPH/Eurographics Symposium on Computer Animation*, San Diego, California, USA, 2007; 191–198.
  22. Muller B, amd Solenthaler M, Keiser R, Gross M. Particle-based fluid–fluid interaction. In *Proceedings of the 2005 ACM SIGGRAPH/Eurographics Symposium on Computer Animation*, Los Angeles, California, USA, 2005; 237–244.
  23. Muller M, Charypar D, Gross M. Particle-based fluid simulation for interactive applications. In *Proceedings of the 2003 ACM SIGGRAPH/Eurographics Symposium on Computer Animation*, San Diego, California, USA, 2003; 154–159.
  24. Cleary P, Pyo S, Prakash M, Koo B. Bubbling and frothing liquids. *ACM Transaction on Graphics* 2007; **26**: 555–564.
  25. Becker M, Teschner M. Weakly compressible sph for free surface flows. *Proceedings of the 2007 ACM SIGGRAPH/Eurographics Symposium on Computer Animation*, San Diego, California, USA, 2007; **9**: 209–217.
  26. Patankar NA. A formulation for fast computations of rigid particulate flows. In *Center for Turbulence Research Annual Research Briefs*, Stanford University, USA, 2001; 185–196.
  27. Sun HQ, Han JQ. Particle-based realistic simulation of fluid–solid interaction. *Computer Animation and Virtual Worlds* 2010; **21**: 589–595.

## AUTHORS' BIOGRAPHIES



**Xuqiang Shao** was born in 1982. He is a PhD student of State Key Laboratory of Virtual Reality Technology and Systems, Beihang University, China, and a student member of China Computer Federation. His main research interests include computer graphics and virtual reality.



**Zhong Zhou** was born in 1978. He is an associate professor of State Key Laboratory of Virtual Reality Technology and Systems, Beihang University, China, and a senior member of China Computer Federation. His main research interests include wireless sensor network, distributed virtual reality and visualization technology.



**Wei Wu** was born in 1961. He is professor of State Key Laboratory of Virtual Reality Technology and Systems, Beihang University, China. He is a senior member of China Computer Federation. His main research interests include wireless sensor network, distributed virtual reality and visualization technology.